ORIGINAL RESEARCH

Laryngoscope
Investigative Otolaryngology

Electrical stimulation of cochlear implant promotes activation of macrophages and fibroblasts under inflammation

Dingling Zhang[1] | Dongxiu Chen[1] | Kaiye Wang[1] | Jing Pan[1] |
Jie Tang PhD[1,2,3,4] | Hongzheng Zhang MD, PhD[1,4] ⓘ

[1]Department of Otolaryngology Head and Neck Surgery, Zhujiang Hospital of Southern Medical University, Guangzhou, China

[2]Department of Physiology, Southern Medical University School of Basic Medical Sciences, Guangzhou, China

[3]Key Laboratory of Mental Health of the Ministry of Education, Southern Medical University, Guangzhou, China

[4]Hearing Research Center, Southern Medical University, Guangzhou, China

Correspondence
Hongzheng Zhang, Department of Otolaryngology Head and Neck Surgery, Zhujiang Hospital of Southern Medical University, Guangzhou, China.
Email: redtrue@smu.edu.cn

Jie Tang, Department of Physiology, Southern Medical University School of Basic Medical Sciences, Guangzhou, China.
Email: jietang@smu.edu.cn

Abstract

Objectives: The implanted electrodes deliver electric signals to spiral ganglion neurons, conferring restored hearing of cochlear implantation (CI) recipients. Postimplantation intracochlear fibrosis, which is observed in most CI recipients, disturbs the electrical signals and impairs the long-term outcome of CI. The macrophages and fibroblasts activation is critical for the development of intracochlear fibrosis. However, the effect of electric stimulation of cochlear implant (ESCI) on the activity of macrophages and fibroblasts was unclear. In the present study, a human cochlear implant was modified to stimulate cultured macrophages and fibroblasts.

Methods: By measuring cellular marker and the expression level of cytokine production, the polarization and activity of macrophages and fibroblasts were examined with or without ESCI.

Results: Our data showed that ESCI had little effects on the morphology, density, and distribution of culturing macrophages and fibroblasts. Furthermore, ESCI alone did not affect the polarization of macrophages or the function of fibroblasts without the treatment of inflammatory factors. However, in the presence of LPS or IL-4, ESCI further promoted the polarization of macrophages, and increased the expression of pro-inflammatory or anti-inflammatory factors, respectively. For fibroblasts, ESCI further increased the collagen I synthesis induced by TGF-β1 treatment. Nifedipine inhibited ESCI induced calcium influx, and hereby abolished the promoted polarization and activation of macrophages and fibroblasts.

Conclusion: Our results suggest that acute inflammation should be well inhibited before the activation of cochlear implants to control the postoperative intracochlear fibrosis. The voltage-gated calcium channels could be considered as the targets for reducing postimplantation inflammation and fibrosis.

Level of Evidence: NA.

KEYWORDS
cochlear implantation, electrical stimulation, fibroblasts, intracochlear fibrosis, macrophages

1 | INTRODUCTION

Hearing loss is one of the most prevalent disabilities around the world. Currently, cochlear implantation (CI) is the most effective treatment to partially restore hearing for patients with profound-to-severe sensorineural hearing loss.[1] Through an electrode array implanted into the cochlea,[2] acoustic signals are transcoded into electrical signals. Therefore, the outcome of CI is largely relying on the effectiveness of the electrical signals delivered by the CI electrodes.

However, as a common complication, postoperative fibrosis in the cochlea impairs the long-term outcome of CI.[3] Fibrous tissue grows up over time, forming a dense fibrous sheath around the CI electrode.[4] It increases the impedance of CI circles, leading to a decreased dynamic range of stimulation[5] and decreased CI battery life.[6] In addition, fibrous tissue obstructs the vibration of cochlear basilar membrane, resulting in further loss of residual hearing.[7] Moreover, cochlear fibrosis is the primary cause of reimplantation.[8] Clinically, glucocorticoids are usually used to prevent postoperative fibrosis.[9] However, its long-term control of fibrosis was not validated for all cases.[10]

Postoperative cochlear fibrosis has been demonstrated relative to surgical trauma and inflammatory responses.[11] However, it is unknown whether electrical stimulation (ES) of cochlear implant (ESCI) affects inflammation and subsequent fibrosis. As an illustration, cardiac pacemaker is a long-term implant. It was observed that more local fibrous tissue was attached to the lead tip, where electrical pulses were released.[12] Similar effects of ES were also observed in implants for tissues.[13–15] Considering the long working term, unique electrical parameters of ESCI,[16] it is presumably relevant to inflammatory response and subsequent fibrosis. Therefore, it is necessary to explore the relationship between electrical stimulation and inflammation and fibrosis, so as to find the possibility of controlling fibrosis.

2 | METHODS AND MATERIALS

2.1 | Cell culture and treatment

The cell lines (L929 and Raw264.7 from ADCC, HEI-OC1 from biofeng) were cultured in medium (DMEM/F12 for L929, DMEM for HEI-OC1, RPMI-1640 for Raw264.7) (Gibco, Grand Island, NY) containing FBS (5% for L929, 10% for HEI-OC1 and Raw264.7) (Gibco, Grand Island, NY) and antibiotics (50 U/mL penicillin–streptomycin for L929 and Raw264.7) (Gibco, Grand Island, NY) in a humidified incubator (37°C for L929 and Raw264.7, 33°C for HEI-OC1) with 5% CO_2. L929 and HEI-OC1 were seeded to a 12-well plate at a density of 2.5×10^4 cells/well (Raw264.7 was seeded at a density of 8×10^4 cells/well).

In some experiments, LPS (lipopolysaccharide, 100 ng/mL, no. L4391-1MG, Sigma, St Louis, MO) or IL-4 (interleukin 4, 40 ng/mL, no. 214-14-5, PEPROTECH, Cranbury, NJ) was added for 24 h to polarize macrophages into M1 or M2. And L929 was added with TGF-β1 (transforming growth factor-β1, 10 ng/mL, no. 763102, Biolegend, San Diego, CA). Nifedipine (10 μg/mL, no. BAY-a-1040, Selleck, Shanghai, China) was added for 12 h.

2.2 | ESCI

In vitro ES of cochlear implant device is modified from the clinical cochlear implant (no. CS-10A, NUROTRON, Hangzhou, Zhejiang, China), the actual device is composed of the cover with electrodes (Figure 1A, (1)), the cell culture plate (Figure 1A, (2)), and connected electronic cochlear converter (Figure 1A, (3)). Every Central Stimulating electrode (CSe) was linked to the microelectrode of the CI, and the Roude Reference electrode (RRe) was linked to the reference

FIGURE 1 Construction of the ESCI in vitro system. (A) The schematic of the ESCI system. Left, the actual device is composed of the cover with electrodes (1), the cell culture plate (2), and the connected CI processor (3). Right, the loop shows the connection of the central stimulating electrode (CSe) and the ring reference electrode (RRe). (B) The schematic of the cell culture based ESCI system. (C) The comfort level (CL) and threshold level (TL) of electrical stimulation in each electrode for CI recipients. The level was expressed in clinical programming units. (D) The actual current measured from our device and the electrodes of implants for CI recipients.
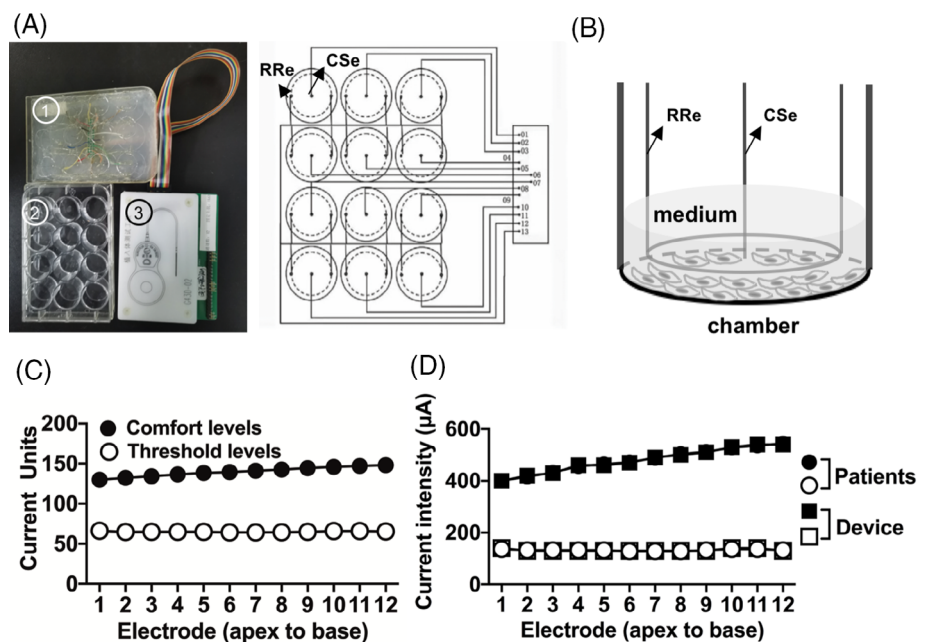
electrode of the cochlear implant. CSe and RRe were made of platinum–iridium wire 0.25 mm in diameter (Figure 1B).

A software Nurosound (NUROTRON, Hangzhou, Zhejiang, China) was used to set the parameters of ESCI. Stereo equipment (SRS-XB12/BC, SONY, Tokyo, Japan) was used to play *Ode to the Motherland* for 12 h continuously per day. The intensity is between 55 and 73 dB, measured by a sound level meter (AS804, SMART SENSOR, Dongguan, Guangdong, China).

2.3 | Cell count

Optical microscopy (Ti-S, Nikon, Shanghai, China) and blood cell counting plate were used for cell counting. The cell distribution counting was counted in an area of 250 μm by 250 μm.

2.4 | Cell counting kit-8 assay

The cells were analyzed by cell counting kit-8 (CCK-8) kit (Dojindo Co. Tokyo, Japan). The plate was determined by the microplate reader (ELX800, BioTek, San Diego, CA).

2.5 | Flow cytometric analysis

Macrophages were analyzed by a PE-CD86 (no. 100113, Biolegend, San Diego, CA) and APC-CD206 staining kit (no. 141705, Biolegend, San Diego, CA) by following the manufacturer's instructions. Flow cytometry was performed on a BD LSRForessa flow cytometer (BD, Franklin, NJ), and the data were analyzed using FlowJo software (FlowJo, Ashland, OR).

2.6 | Quantitative real-time polymerase chain reaction

Total RNA was extracted with Trizol reagent (no. R401-01, Vazyme, Nanjing, Jiangsu, China) according to the manufacturer's instructions. Quantitative real-time polymerase chain reaction (qRT-PCR) was performed using the SYBR Green qRT-PCR kit (no. Q111-02, Vazyme, Nanjing, Jiangsu, China) on a QuantStudioTM 1 Real-Time PCR Instrument (ABI, Waltham, MA). See Table 1 for primers and sequences (Tsingke, Beijing, China). The C_t values were analyzed using the $\Delta\Delta C_t$ method, and the relative quantification of the expression of the target genes was measured using β-actin mRNA as an internal control.

2.7 | ELISA assay

The levels of TGF-β1 released from macrophages were measured using an ELISA kit (no. EK981-96, Multisciences, Hangzhou, Zhejiang,

TABLE 1   All primer and sequences used in the qPCR process.

ID	Primer	Sequence (5′ to 3′)
1	IL-12b forward	GTCCTCAGAAGCTAACCATCTCC
2	IL-12b reverse	CCAGAGCCTATGACTCCATGTC
3	TNF-α forward	CCCTCACACTCAGATCATCTTCT
4	TNF-α reverse	GCTACGACGTGGGCTACAG
5	IL-6 forward	TAGTCCTTCCTACCCCAATTTCC
6	IL-6 reverse	TTGGTCCTTAGCCACTCCTTC
7	IL-10 forward	GCTCTTACTGACTGGCATGAG
8	IL-10 reverse	CGCAGCTCTAGGAGCATGTG
9	TGF-β forward	CTCCCGTGGCTTCTAGTGC
10	TGF-β reverse	GCCTTAGTTTGGACAGGATCTG
11	Arg-1 forward	CTCCAAGCCAAAGTCCTTAGAG
12	Arg-1 reverse	AGGAGCTGTCATTAGGGACATC
13	β-actin forward	CGTTGACATCCGTAAAGACC
14	β-actin reverse	TAGAGCCACCAATCCACACA

China). The plate was determined by the microplate reader (ELX800, BioTek, San Diego, CA).

2.8 | Western blot

The protein was extracted from cultured cells with cell lysis buffer (no. P0013, beyotime, Shanghai, China). A total of 30 μg protein sample was separated by SDS–PAGE gels and transferred to a polyvinylidene fluoride (PVDF) membrane (Millipore, Bedford, MA). After blocking with 5% non-fat milk in TBS-T (Beyotime, Shanghai, China) for 2 h at RT, the membrane was incubated with the primary antibodies collagen I (no. AB755P, Sigma, St. Louis, MO) overnight at 4°C. The PVDF membrane was washed and incubated with secondary antibodies conjugated to the HRP (BBI Life Sciences, Shanghai, China) for 2 h. Species-matched horseradish peroxidase-conjugated IgG was used as the secondary antibody. Protein bands were detected with a chemiluminescence detection system (Image 600, GE Healthcare, Chicago, IL). Grayscale was analyzed with the software Image Quant TL (GE Healthcare, Chicago, IL). And the relative quantification of the expression of Collagen I was measured using glyceraldehyde-3-phosphate dehydrogenase (GAPDH) as an internal control.

2.9 | Calcium imaging

Rhod-2AM, a cell permeable (1 μM, no. 40776ES50, Yeason, Shanghai, China) fluorescence was utilized to determine intracellular calcium levels. Cells were washed three times with Ca^{2+}-free HBSS (no. H1046, Solarbio, Beijing, China), and Rhod-2 was added for 60 min. After incubation, cells were washed three times in HBSS (no. H1025, Solarbio, Beijing, China). The emitted fluorescence

intensity of Rhod-2 was recorded on Confocal microscopy (FV3000, OLYMPUS, Tokyo, Japan) at 25°C (excitation 549 nm, emission 578 nm). Ionomycin (1 μM, no. S48414, Yuanye, Shanghai, China) is used to get extracellular calcium into cells. Images were analyzed using the software Image Quant TL (GE Healthcare, Chicago, IL).

2.10 | Statistical analysis

SPSS 21.0 (IBM SPSS Inc. Chicago, IL) statistical software was used to analyze the data. The measurement data were expressed as mean ± standard deviation (error). The unpaired Student's t-test was used to compare the data with normal distribution and variance
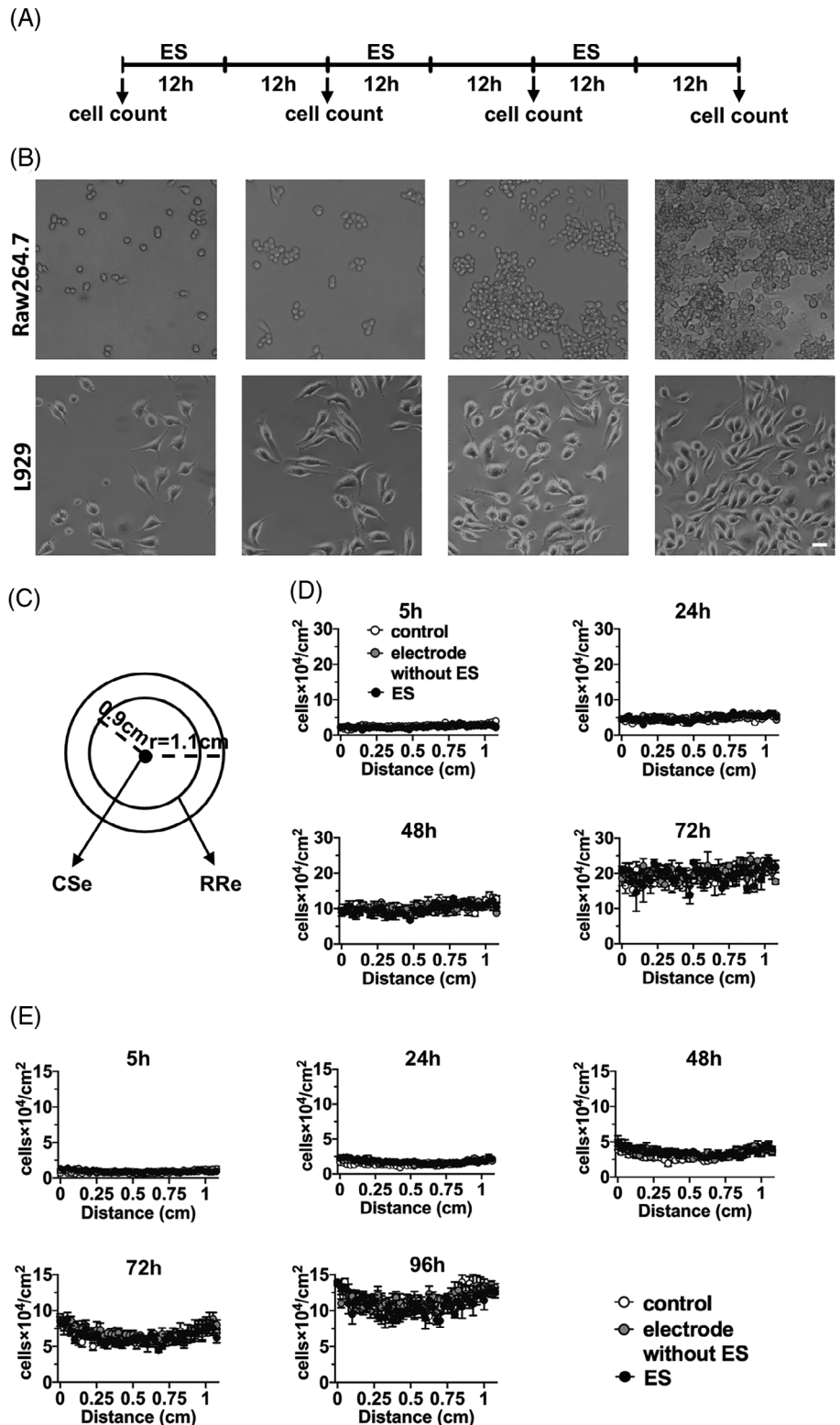
FIGURE 2 The effect of ESCI on the culturing macrophages and fibroblasts. (A) Schematic diagram of the experiment. Electrical stimulation (ES) was performed for 12 h/day until the cells filled the chamber. (B) Representative photographs show the Raw264.7 macrophages and L929 fibroblasts before and after electrical stimulation. Scale bar = 10 μm. (C) Schematic of the stimulation electrodes. The cell density was measured from the CSe to the edge of the culture chamber ($n = 3$ for each group). (D) The distribution and density of macrophages at different time after ESCI. (E) The distribution and density of fibroblasts at different time after ESCI ($n = 3$ for each group). Data were present as mean ± SD.

homogeneity between the two groups. The one-way analysis of variance (ANOVA) was utilized to analyze the data among multiple groups, and the data at different time points were analyzed by repeated ANOVA (Tukey's post hoc test). $p < .05$ indicates significant difference. The diagram is drawn using GraphPad Prism 8 (San Diego, CA).

3 | RESULTS

To examine the possible impairment of ESCI on the inner ear cells, ES converted from sound signals was delivered to cultured HEI-OC1 cells through a human CI device (Figure 1A,B). The ES used in our experiment was compared with the parameters used for CI patients. For each microelectrode, the range of stimulus intensity level was set between the threshold level (TL: the minimum value of stimulation that elicited a very soft, but consistent, hearing sensation) and the

comfort level (CL: the maximum value of stimulation that did not produce uncomfortably loud sounds) (Figure 1C and Ref. [16]). The actual current levels measured from our stimulus electrodes were coincidental with those of the levels measured from CI (Figure 1D). These results indicate that the ES used in our experiment was comparable to that in the cochlea of CI patients.

Under the ES, the cells grew well and filled the chamber within 72 h, without any obvious mortality and abnormal shapes were observed (see Figure S1a). And the cell density and viability was not affected by the presence of electrodes or ES (see Figure S1b,c). Together with the measurements of electrical parameters, these data suggest that the ES of the CI device is safe for the cells in our experiments.

The macrophages and fibroblasts play major roles in the process of fibrosis after CI. The effect of ESCI on cell growth was first examined for Raw264.7, a macrophage cell line, and L929, a fibroblast cell line (Figure 2A,B, and see Figure S2a–c). As shown in Figure 2C, the
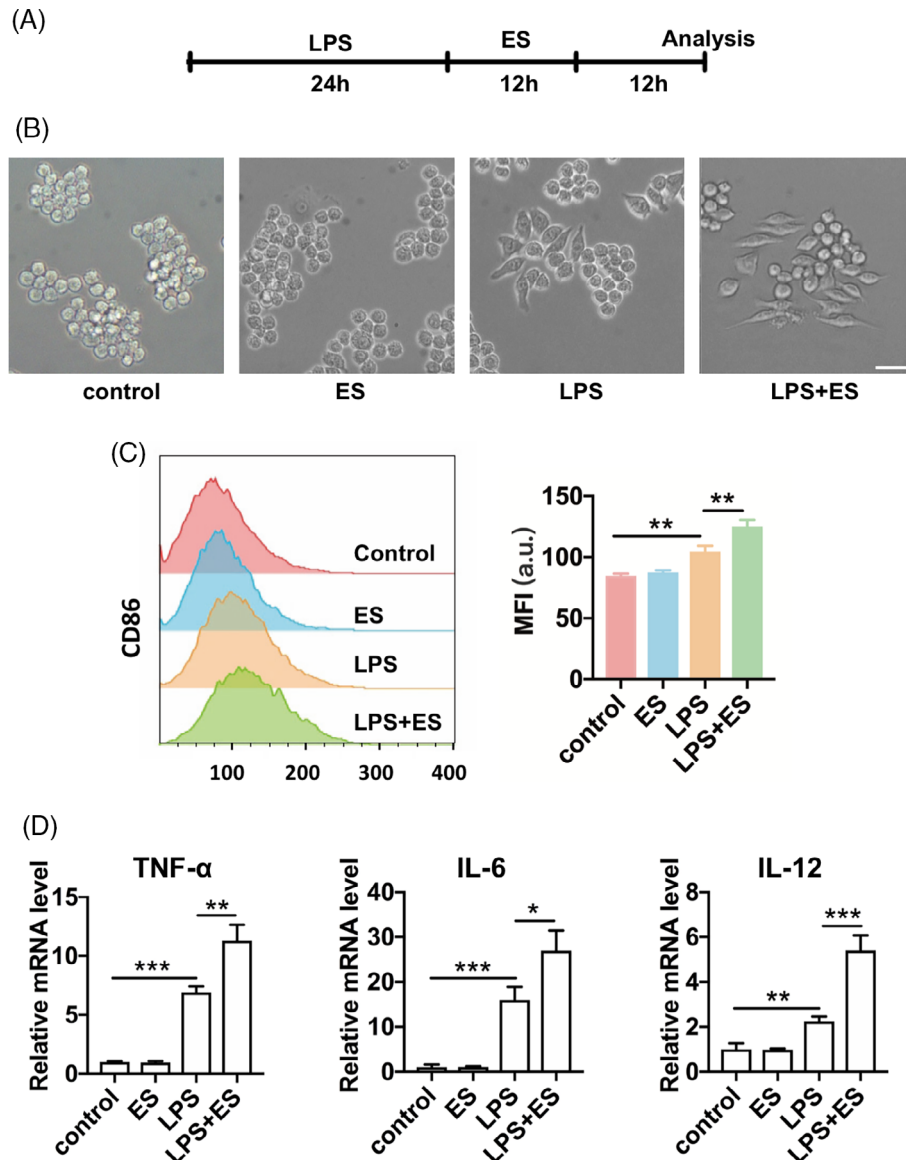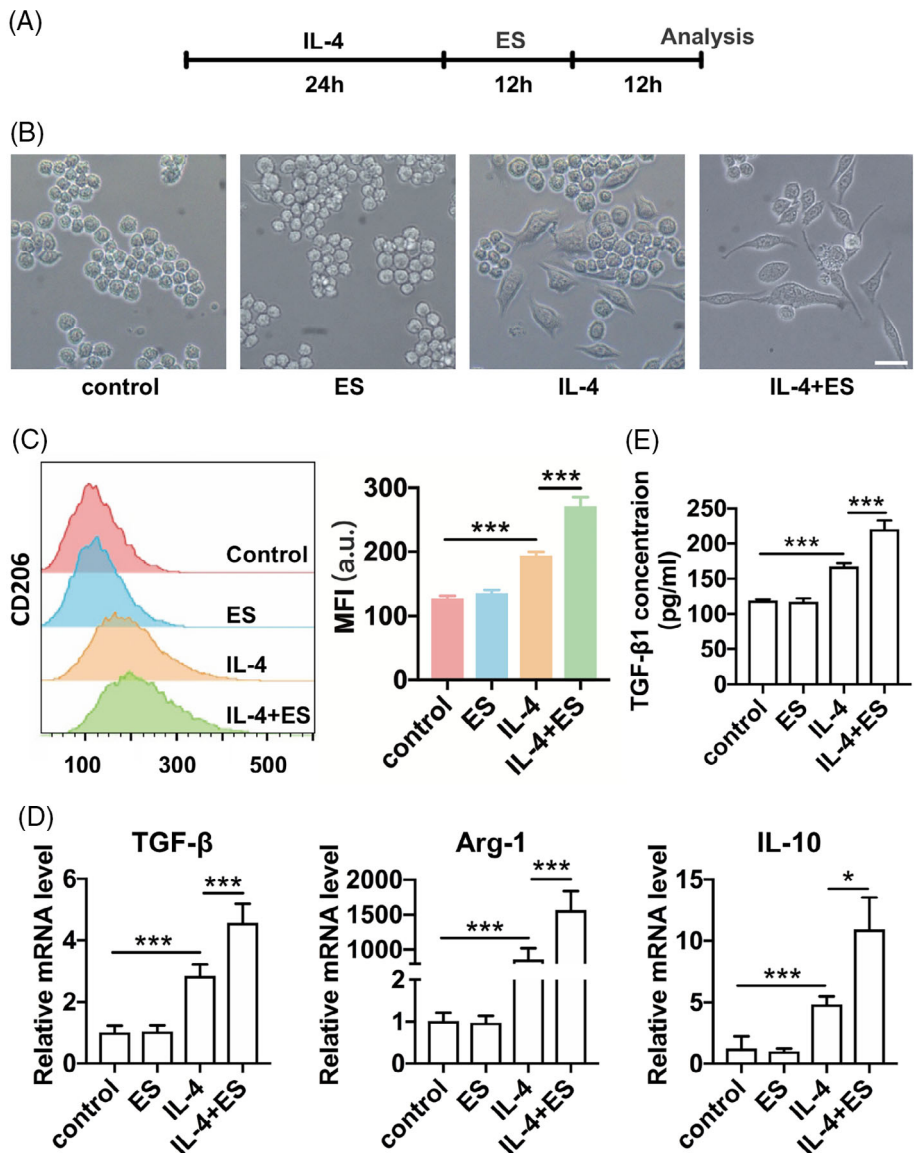

FIGURE 3 The effects of ESCI on LPS-treated macrophages. (A) Schematic diagram of the experiment. (B) Representative photographs show the macrophages in control, electrical stimulation (ES) only, LPS treatment only, and LPS and ES co-treatment group. Scale bar = 10 μm. (C) Flow cytometry assay shows quantitative changes of CD86 fluorescence in macrophages from each group. MFI: mean fluorescence intensity ($n = 3$ for each group). (D) Relative mRNA levels of TNF-α, IL-6, and IL-12 in macrophages from each group ($n = 3$ for each group). Data were present as mean ± SD. ***$p < .001$; **$p < .01$; *$p < .05$, Student's t-test.

possible migration of cells was determined by the cell distribution along the axis from the central stimulating electrode to the edge of the chamber (reference electrode). Compared with the controls, the density and the distribution of the macrophages (Figure 2D) and fibroblasts (Figure 2E) were not disturbed by the presence of electrodes or ES at all periods of ESCI. Thus, we conclude that ES does not affect the proliferation and distribution of macrophages and fibroblasts in the non-inflammatory state.

The surgical trauma and postoperative infection cause acute inflammation in the cochlea after CI.[17,18] The activities of immunocytes, in particular with the M1 macrophages mediate the pro-inflammatory effect.[19] In the present study, LPS was added to mimic acute postoperative inflammation in vitro (Figure 3A). In line with the results of HEI-OC1 cells, ESCI only rarely changed the shape of cultured macrophages, which showed round bodies and scarce dendrites (Figure 3B, ES). Meanwhile, under the administration of LPS, some of the macrophages showed ameboid deformations, indicating the

polarization to M1 (Figure 3C, LPS). Interestingly, in the presence of LPS administration, obvious amoebic changes were observed in more macrophages showing prominent pseudopodia (Figure 3C, LPS + ES) under the ESCI. Flow cytometry data showed that the expression of CD86, a typical M1 marker, was further increased by the co-treatment of ES and LPS (Figure 3C). In addition, the expression of M1 pro-inflammatory cytokines, such as tumor necrosis factor-α (TNF-α), interleukin 6 (IL-6), and interleukin 12 (IL-12), was also further increased by ESCI (Figure 3D). These results suggested that ES promoted the activity of M1 and its pro-inflammatory function.

Because of the foreign body response elicited by CI electrodes in the cochlea, chronic inflammation was usually observed after CI surgery.[17] The M2 of macrophage plays a role in tissue repair and anti-inflammatory effect.[19] To determine the effects of ESCI on M2, IL-4 was used to stimulate macrophages to the M2 (Figure 4A). In line with previous study,[20] we found that macrophages were elongated and showed spindle shapes after IL-4 stimulation, indicating polarization

FIGURE 4 The effects of ESCI on IL-4 treated macrophages. (A) Schematic diagram of the experiment. (B) Representative photographs show the macrophages in control, electrical stimulation (ES) only, IL-4 treatment only, and IL-4 and ES co-treatment group. Scale bar = 10 μm. (C) Flow cytometry assay shows quantitative changes in CD206 fluorescence in macrophages from each group. MFI: mean fluorescence intensity (n = 3 for each group). (D) Relative mRNA levels of TGF-β, Arg-1, and IL-10 in macrophages from each group (n = 3 for each group). (E) ELISA assay shows the concentration of TGF-β1 in the medium from each group (n = 3 for each group). Data were present as mean ± SD. ***p < .001; *p < .05, Student's t-test.

to M2. With the application of IL-4, ESCI made more macrophages showing M2 morphology with flattened cell bodies and elongated pseudopodia (Figure 4B). We chose CD206, a classic M2 marker, to quantify this change by flow cytometry assay. Data showed that ESCI significantly increased the polarization of the M2 (Figure 4C). Functionally, compared with the treatment of IL-4 only, co-treatment of ESCI and IL-4 significantly increased the expression of anti-inflammatory cytokines, such as TGF-β, arginase-1 (Arg-1), and interleukin 10 (IL-10) (Figure 4D). Notably, more TGF-β1 was also detected in the culture medium for the co-treatment of ESCI and IL-4 (Figure 4E).

Our previous study has confirmed that M2 secreted TGF-β1 results in the increasing formation of extracellular matrix.[9] In most cases, a fibrous sheath riching of extracellular matrix was formed around the implanted electrode.[21] As shown in Figure 5A, L929 cells treated with TGF-β1 synthesized more collagen I compared with the control, while ES alone did not affect the ability to synthesize collagen I. Amazingly, the ability of L929 cells to synthesize collagen I was further enhanced by ES under the administration of TGF-β1 (Figure 5B,C). Thus, we concluded that ES not only indirectly induced fibroblast migration and activation by stimulating M2 to secrete TGF-

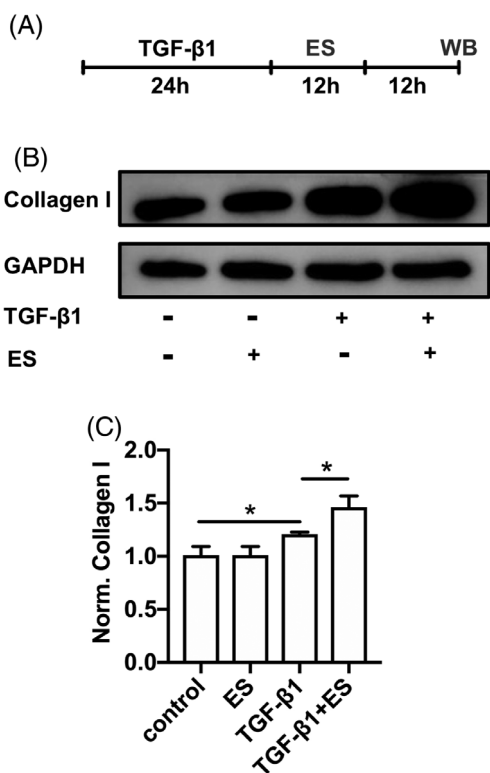β1 but also directly stimulated L929 cells to synthesize more collagen, thereby exacerbating fibrosis.

ESCI activates the voltage-gated sodium and potassium channels of cochlear ganglion neurons, resulting in the excitation of the auditory pathway. Meanwhile, such ES may also act on the ion channels, for example, voltage-activated calcium channels, of other cells in the cochlea. The calcium, which acts as a typical second messenger, has been demonstrated to regulate the function of many cell types, including macrophages[22] and fibroblasts.[23] To examine the role of ESCI elicited calcium influx in the activities of macrophages and fibroblasts, the voltage-gated calcium channel blocker, nifedipine, was applied after IL-4 or TGF-β1 treatment (Figure 6A). Administrated by nifedipine alone, the cell viability, proliferation, and cell shapes of macrophages and fibroblasts were not changed by a concentration of 10 μg/mL (see Figure S3). As shown by the data of flow cytometry assay in Figure 6B, compared with the IL-4 treated group, the mean fluorescence intensity of CD206 labeled M2 increased by IL-4 and ESCI co-treatment. However, the increase of M2 by ESCI was abolished by nifedipine, while nifedipine treatment alone made no difference. Moreover, the increased expression of anti-inflammatory cytokines, including TGF-β, Arg1, and IL-10, by ESCI and IL-4 co-treatment was also reduced significantly by nifedipine (Figure 6C and see Figure S4a). These results indicate that the promotion of M2 polarization by ESCI was significantly intercepted by nifedipine. Likewise, nifedipine reduced the increase of collagen I expression induced by ES in fibroblasts (Figure 6D,E and see Figure S4b,c). These results indicate that nifedipine can not only reduce the secretion of TGF-β of M2 macrophages but also directly act on L929 cells to inhibit their collagen synthesis function.

To further confirm the calcium influx, we used fluorescent probe Rhod2-AM to examine the intracellular calcium level of IL-4 pre-incubated Raw264.7 in response to ESCI. As shown in Figure 7A, ESCI elicited a robust increase in intracellular calcium levels (red lines). In line with the results shown in Figure 6, nifedipine almost abolished this calcium influx (Figure 7B,C). A similar calcium influx elicited by ESCI was also observed in TGF-β1 pretreated L929 cells (Figure 7D–F). These results demonstrated that ESCI induced calcium influx via the voltage-gated calcium channels on the macrophages and fibroblasts.

FIGURE 5 The effects of ESCI on TGF-β1 treated fibroblasts. (A) Schematic diagram of experiment. (B) The West-blotting bands show the expression level of collagen I in control, electrical stimulation (ES) only, TGF-βtreatment only, and TGF-βand ES co-treatment group. (C) Normalized expression level of collagen I in each group (n = 3 for each group). Data were present as mean ± SD. *p < .05, Student's t-test.

4 | DISCUSSION

In the early stage after cochlear implantation, acute inflammation often occurs due to surgical trauma and infection.[24,25] Upon injury, proteins near the surgical path adhere to the surface of the electrode.[26] Then, the inflammatory factors released from the dying cells induce immunocytes to migrate around the electrode.[27] Monocytes are one of the immunocytes that are involved in these acute immune responses.[28] Infection caused monocytes to polarize into M1.[29] M1 secrets IL-6/IL-12/TNF-α and so on and plays a major role in promoting inflammation and phagocytosis.[19] It can be also observed in cultured cell lines treated by bacterial cell wall component LPS

FIGURE 6 Nifedipine abolished the promoting effects of ESCI on treated macrophages and fibroblasts. (A) Schematic diagram of experiment. (B) Flow cytometry assay shows quantitative changes in CD206 fluorescence in macrophages from each group. MFI: mean fluorescence intensity ($n = 3$ for each group). (C) Relative mRNA levels of TGF-β, Arg-1, and IL-10 in macrophages from each group ($n = 3$ for each group). (D) The West-blotting bands show the expression level of collagen I from fibroblasts in each group. (E) Normalized expression level of collagen I in each group ($n = 3$ for each group). Data were present as mean ± SD. ns, no statistical difference; ***$p < .001$; **$p < .01$; *$p < .05$, Student's t-test.
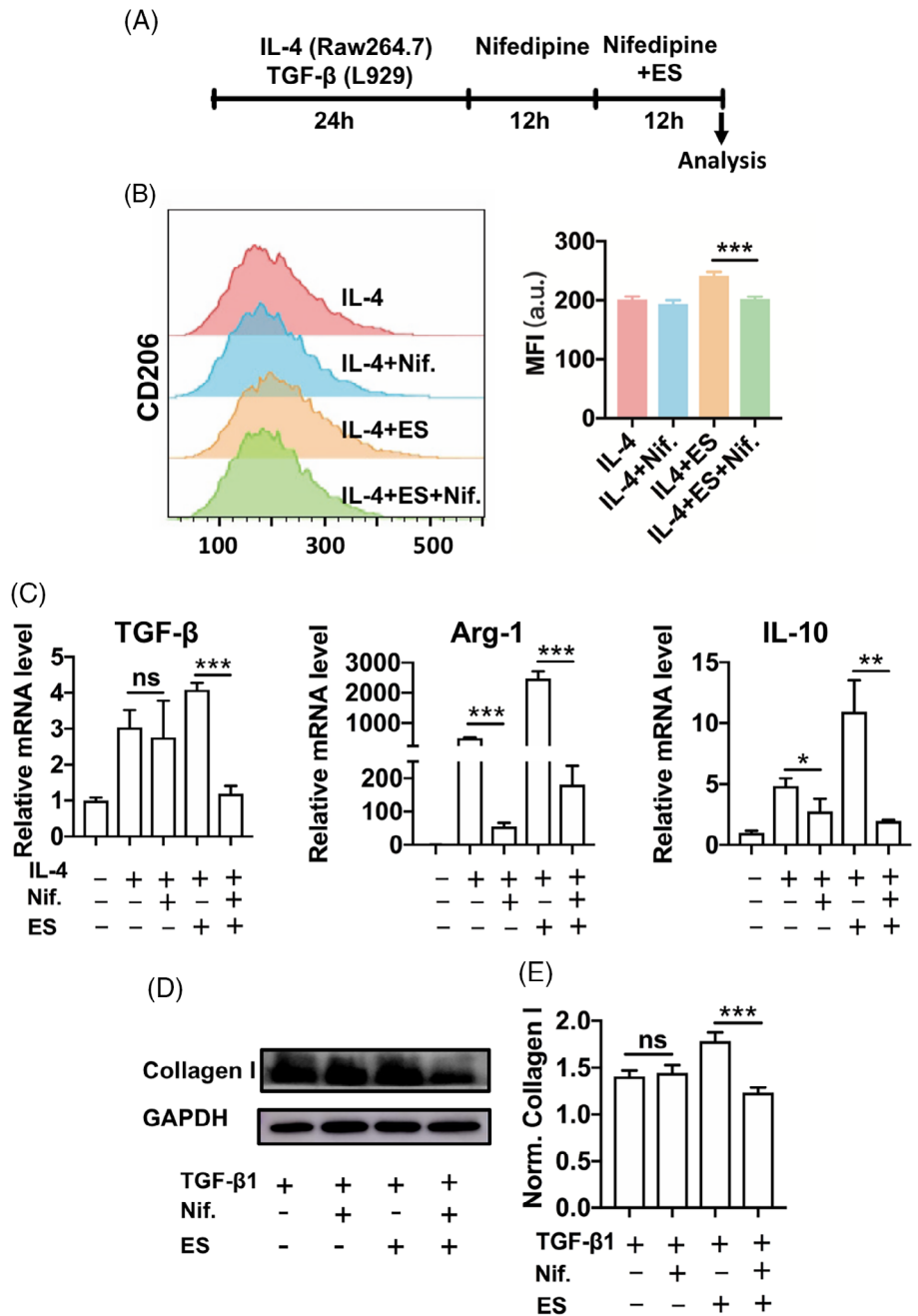

(Figure 3). Excessive acute inflammatory response results in damage to cochlear cells and delays wound healing.[30] Clinically, glucocorticoid therapy is usually employed to reduce the acute inflammatory responses after CI.[31]

In the presence of CI electrode, chronic inflammation is always occurred in the cochlea.[25] M1 transformed into the M2 gradually,[32] and newly migrated macrophages can be polarized to M2 by IL-4, which was also used to induce M2 in our experiment. Cytokine including TGF-β and IL-10 are secreted and act primarily as anti-inflammatory factors and promote tissue repair (Figure 4). Under the action of TGF-β1, the fibroblasts are recruited and activated into myofibroblasts around the CI electrodes (Figure 5). Large amounts of collagen and other extracellular matrix are synthesized and secreted to repair damaged tissue.[33] However,

overactivated fibroblasts can form a fibrous sheath around the CI electrodes.[34] In 90% of temporal bone specimens of patients receiving cochlear implantation, fibrous tissue is found wrapping around the implanted electrode.[35,36] The fibrous sheath around the electrode leads to poor accuracy of ES[5] and a high possibility of reimplantation.[37] At present, effective treatment specialized for cochlear fibrous after CI is not well developed.

A distinct feature of cochlear implants is the ES following cochlear implantation. The chronic effects of ES on inflammation and intracochlear fibrosis remain debatable. In the research of cardiac pacemakers and wound healing, ES is one of the independent factors promoting fibrosis.[12,15] There is thicker fibrous tissue in the discharge part than in the other parts. Cochlear implants also work with electrical impulses. By impedance measurement, the electrode functionality
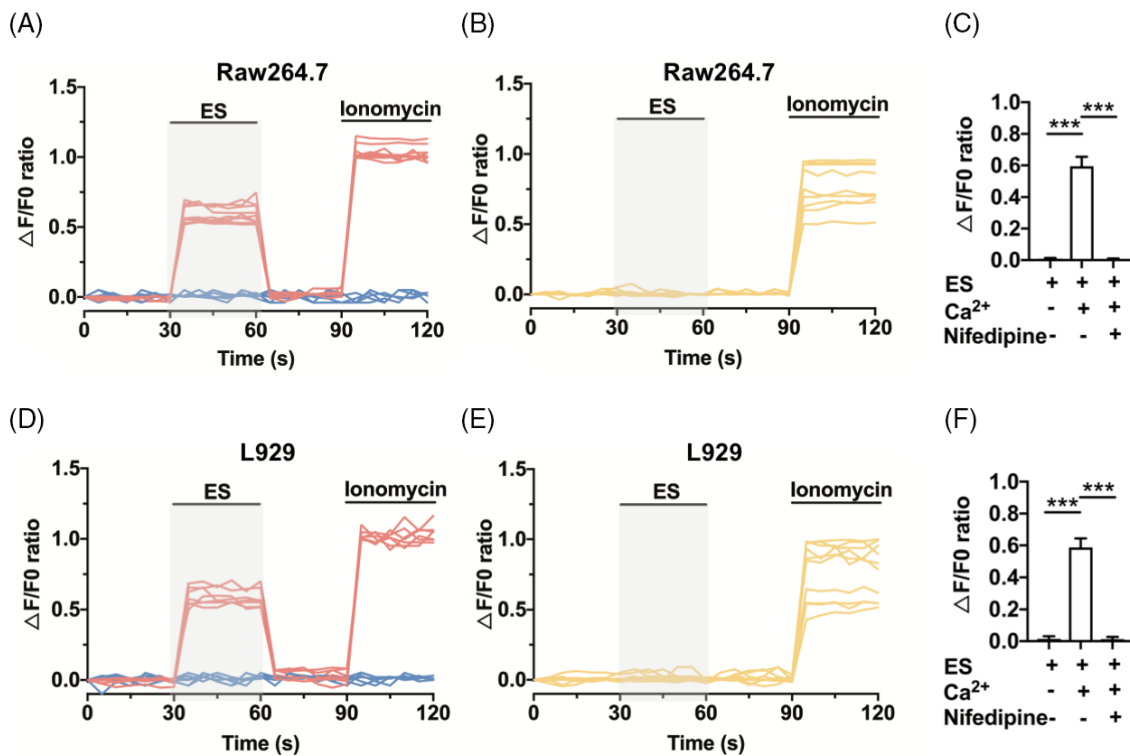
FIGURE 7 The effects of ESCI on calcium influx in macrophages and fibroblasts. (A) The intracellular calcium fluorescence of IL-4 treated macrophages was measured in normal (red, $n = 9$) or Ca^{2+}-free ($n = 5$) medium. The gray area shows the period of electrical stimulation. Ionomycin, a calcium ionophore, was used as the positive control. (B) The intracellular calcium fluorescence of IL-4 treated macrophages under the administration of nifedipine ($n = 9$). (C) The average fluorescence level in gray areas of A and B. (D) The intracellular calcium fluorescence of TGF-β1 treated fibroblasts measured in normal (red, $n = 7$) or Ca^{2+}-free ($n = 6$) medium. (E) The intracellular calcium fluorescence of TGF-β1 treated fibroblasts under the administration of nifedipine ($n = 9$). (F) The average fluorescence level in gray are of D and E. Data were present as mean ± SD. ***$p < .001$, Student's t-test.

loss time of the ES group was shorter than that of a non-stimulation group.[38] In addition, in guinea pig cochlea, chronic ES at high charge densities evoked a vigorous tissue response and increased Pt electrode dissolution compared with Pt electrodes only.[39] Conversely, it has been reported that electric stimulation does not cause CX3CR1+ macrophages to migrate into the mouse cochlea.[40] Our in vitro results showed that electric stimulation did not induce migration and promoted the activity of macrophage and fibroblasts in the absence of inflammatory factors (Figures 2–5). However, in the presence of inflammatory factors, our study indicates that ESCI leads to greater early pro-inflammatory function and later pro-repair function by promoting further polarization of macrophages (Figures 3 and 4).

Voltage-gated calcium channels are widespread in non-excitable cells including macrophages and fibroblasts, serving as one of the effectors for the perception of external ES in these cells.[41,42] While exciting spiral ganglion neurons, ESCI is sufficient to open voltage-gated calcium channels on macrophages and fibroblasts and cause calcium influx (Figure 7). As a second messenger, intracellular calcium concentration is involved in the activation of macrophages and fibrosis.[43,44] Intracellular calcium regulates the conformational state of calmodulin[45] resulting in the polarization of macrophages.[46] Classical TGF-β signaling and the downstream transcription factors such as Smad2/3 are phosphorylated, and then the genes

related to fibrosis are activated.[47] Increased intracellular calcium activates calmodulin binding with Smad2, thereby activating the pathway.[48] In addition, calcium can regulate other fibrosis-related pathways to play a role in promoting repair directly.[23] Therefore, we proposed a reasonable conjecture that postimplantation fibrosis is promoted by the calcium influx through the ESCI-activated calcium channels.

The limitation of this study is that it still stays in the cell experiment stage and only uses a single stimulus factor to simulate different stages after surgery. However, the internal environment of the cochlea after surgery is complex and there are many influencing factors, and the impact of ES on the cells in the cochlea is still unknown. Therefore, in vivo experiments should be supplemented in the future. In addition, how ES opens voltage-gated calcium channels and the effects of intracellular signaling pathways have not been explored, and continued research may find more precise regulatory targets for the prevention and treatment of fibrosis.

5 | CONCLUSION

According to the updated guidelines, the activation day of a cochlear implant is recommended at 1–6 weeks (U.S. FDA and Ref. [49]) after

surgery. Our in vitro results suggest that it may fully consider determining the activation time for individual CI recipients until the acute inflammation subsides. In addition, long-term foreign body responses and chronic inflammation should also be considered. ES, as an independent physical factor, may promote chronic inflammation.

ACKNOWLEDGMENTS

CONFLICT OF INTEREST STATEMENT

The authors declare that they have no conflict of interest.

ORCID

Hongzheng Zhang 🄳 https://orcid.org/0000-0001-8105-2256

REFERENCES

1. Kitterick PT, Smith SN, Lucas L. Hearing instruments for unilateral severe-to-profound sensorineural hearing loss in adults: a systematic review and meta-analysis. *Ear Hear*. 2016;37(5):495-507.
2. Mowry SE, Woodson E. Cochlear implant surgery. *JAMA Otolaryngol Head Neck Surg*. 2020;146(1):92.
3. Jensen MJ, Claussen AD, Higgins T, et al. Cochlear implant material effects on inflammatory cell function and foreign body response. *Hear Res*. 2022;426:108597.
4. Colesa DJ, Devare J, Swiderski DL, Beyer LA, Raphael Y, Pfingst BE. Development of a chronically-implanted mouse model for studies of cochlear health and implant function. *Hear Res*. 2021;404:108216.
5. Caswell-Midwinter B, Doney EM, Arjmandi MK, Jahn KN, Herrmann BS, Arenberg JG. The Relationship Between Impedance, Programming and Word Recognition in a Large Clinical Dataset of Cochlear Implant Recipients. *Trends Hear*. 2022;26:23312165211060983.
6. Maruthurkkara S, Allen A, Cullington H, Muff J, Arora K, Johnson S. Remote check test battery for cochlear implant recipients: proof of concept study. *Int J Audiol*. 2022;61(6):443-452.
7. Tejani VD, Yang H, Kim JS, et al. Access and polarization electrode impedance changes in electric-acoustic stimulation cochlear implant users with delayed loss of acoustic hearing. *J Assoc Res Otolaryngol*. 2022;23(1):95-118.
8. Lane C, Zimmerman K, Agrawal S, Parnes L. Cochlear implant failures and reimplantation: a 30-year analysis and literature review. *Laryngoscope*. 2020;130(3):782-789.
9. Chen D, Luo Y, Pan J, et al. Long-term release of dexamethasone with a Polycaprolactone-coated electrode alleviates fibrosis in cochlear implantation. *Front Cell Dev Biol*. 2021;9:740576.
10. Skarżyńska MB, Kołodziejak A, Gos E, et al. The clinical effect of steroids for hearing preservation in cochlear implantation: conclusions based on three cochlear implant systems and two administration regimes. *Pharmaceuticals (Basel)*. 2022;15(10):1176.
11. Jia H, François F, Bourien J, et al. Prevention of trauma-induced cochlear fibrosis using intracochlear application of anti-inflammatory and antiproliferative drugs. *Neuroscience*. 2016;316:261-278.
12. Rennert RC, Rustad K, Levi K, et al. A histological and mechanical analysis of the cardiac lead-tissue interface: implications for lead extraction. *Acta Biomater*. 2014;10(5):2200-2208.
13. Han N, Xu CG, Wang TB, et al. Electrical stimulation does not enhance nerve regeneration if delayed after sciatic nerve injury: the role of fibrosis. *Neural Regen Res*. 2015;10(1):90-94.
14. Pinheiro-Dardis CM, Russo TL. Electrical stimulation based on chronaxie increases fibrosis and modulates TWEAK/Fn14, TGF-β/Myostatin, and MMP pathways in denervated muscles. *Am J Phys Med Rehabil*. 2017;96(4):260-267.
15. Luo R, Dai J, Zhang J, Li Z. Accelerated skin wound healing by electrical stimulation. *Adv Healthc Mater*. 2021;10(16):e2100557.
16. Zeng FG, Rebscher SJ, Fu QJ, et al. Development and evaluation of the Nurotron 26-electrode cochlear implant system. *Hear Res*. 2015; 322:188-199.
17. Foggia MJ, Quevedo RV, Hansen MR. Intracochlear fibrosis and the foreign body response to cochlear implant biomaterials. *Laryngoscope Investig Otolaryngol*. 2019;4(6):678-683.
18. Davidson L, Foley DA, Clifford P, et al. Infectious complications and optimising infection prevention for children with cochlear implants. *J Paediatr Child Health*. 2022;58(6):1007-1012.
19. Yunna C, Mengru H, Lei W, Weidong C. Macrophage M1/M2 polarization. *Eur J Pharmacol*. 2020;877:173090.
20. Shapouri-Moghaddam A, Mohammadian S, Vazini H, et al. Macrophage plasticity, polarization, and function in health and disease. *J Cell Physiol*. 2018;233(9):6425-6440.
21. Swiderski DL, Colesa DJ, Hughes AP, Raphael Y, Pfingst BE. Relationships between Intrascalar tissue, neuron survival, and cochlear implant function. *J Assoc Res Otolaryngol*. 2020;21(4):337-352.
22. Tabei Y, Sugino S, Eguchi K, et al. Effect of calcium carbonate particle shape on phagocytosis and pro-inflammatory response in differentiated THP-1 macrophages. *Biochem Biophys Res Commun*. 2017; 490(2):499-505.
23. Subramaniam T, Fauzi MB, Lokanathan Y, Law JX. The role of calcium in wound healing. *Int J Mol Sci*. 2021;22(12):6486.
24. Ryu KA, Lyu AR, Park H, Choi JW, Hur GM, Park YH. Intracochlear bleeding enhances cochlear fibrosis and ossification: an animal study. *PloS One*. 2015;10(8):e0136617.
25. Rahman MT, Chari DA, Ishiyama G, et al. Cochlear implants: causes, effects and mitigation strategies for the foreign body response and inflammation. *Hear Res*. 2022;422:108536.
26. Weiskirchen R, Weiskirchen S, Tacke F. Organ and tissue fibrosis: molecular signals, cellular mechanisms and translational implications. *Mol Aspects Med*. 2019;65:2-15.
27. Nourshargh S, Alon R. Leukocyte migration into inflamed tissues. *Immunity*. 2014;41(5):694-707.
28. Wynn TA, Vannella KM. Macrophages in tissue repair, regeneration, and fibrosis. *Immunity*. 2016;44(3):450-462.
29. Gordon S, Martinez FO. Alternative activation of macrophages: mechanism and functions. *Immunity*. 2010;32(5):593-604.
30. Tracey KJ. The inflammatory reflex. *Nature*. 2002;420(6917): 853-859.
31. Cortés Fuentes IA, Videhult Pierre P, Engmér BC. Improving clinical outcomes in cochlear implantation using glucocorticoid therapy: a review. *Ear Hear*. 2020;41(1):17-24.
32. Smigiel KS, Parks WC. Macrophages, wound healing, and fibrosis: recent insights. *Curr Rheumatol Rep*. 2018;20(4):17.
33. Wang PH, Huang BS, Horng HC, Yeh CC, Chen YJ. Wound healing. *J Chin Med Assoc*. 2018;81(2):94-101.
34. Buswinka CJ, Colesa DJ, Swiderski DL, Raphael Y, Pfingst BE. Components of impedance in a cochlear implant animal model with TGFβ1-accelerated fibrosis. *Hear Res*. 2022;426:108638.
35. Seyyedi M, Nadol JB Jr. Intracochlear inflammatory response to cochlear implant electrodes in humans. *Otol Neurotol*. 2014;35(9): 1545-1551.
36. Kamakura T, Nadol JB Jr. Correlation between word recognition score and intracochlear new bone and fibrous tissue after cochlear implantation in the human. *Hear Res*. 2016;339:132-141.

37. Yao X, Liu H, Si J, Ding X, Zhao Y, Zheng Y. Research status and future development of cochlear reimplantation. *Front Neurosci*. 2022; 16:824389.

38. Claussen AD, Vielman Quevedo R, Mostaert B, Kirk JR, Dueck WF, Hansen MR. A mouse model of cochlear implantation with chronic electric stimulation. *PloS One*. 2019;14(4):e0215407.

39. Shepherd RK, Carter PM, Enke YL, Wise AK, Fallon JB. Chronic intra-cochlear electrical stimulation at high charge densities results in platinum dissolution but not neural loss or functional changes in vivo. *J Neural Eng*. 2019;16(2):026009.

40. Claussen AD, Quevedo RV, Kirk JR, et al. Chronic cochlear implantation with and without electric stimulation in a mouse model induces robust cochlear influx of CX3CR1(+/GFP) macrophages. *Hear Res*. 2022;426:108510.

41. Antony C, Mehto S, Tiwari BK, Singh Y, Natarajan K. Regulation of L-type voltage gated calcium channel CACNA1S in macrophages upon mycobacterium tuberculosis infection. *PloS One*. 2015;10(4): e0124263.

42. Sadras F, Stewart TA, Robitaille M, et al. Altered calcium influx pathways in cancer-associated fibroblasts. *Biomedicine*. 2021;9(6):680.

43. Janssen LJ, Mukherjee S, Ask K. Calcium homeostasis and ionic mechanisms in pulmonary fibroblasts. *Am J Respir Cell Mol Biol*. 2015;53(2): 135-148.

44. Zhao X, Kong Y, Liang B, et al. Mechanosensitive Piezo1 channels mediate renal fibrosis. *JCI Insight*. 2022;7(7):e152330.

45. Chin D, Means AR. Calmodulin: a prototypical calcium sensor. *Trends Cell Biol*. 2000;10(8):322-328.

46. Mu G, Zhu Y, Dong Z, Shi L, Deng Y, Li H. Calmodulin 2 facilitates angiogenesis and metastasis of gastric cancer via STAT3/HIF-1A/VEGF-a mediated macrophage polarization. *Front Oncol*. 2021;11:727306.

47. Peng D, Fu M, Wang M, Wei Y, Wei X. Targeting TGF-β signal transduction for fibrosis and cancer therapy. *Mol Cancer*. 2022; 21(1):104.

48. Ming M, Manzini I, Le W, Krieglstein K, Spittau B. Thapsigargin-induced Ca2+ increase inhibits TGFβ1-mediated Smad2 transcriptional responses via Ca2+/calmodulin-dependent protein kinase II. *J Cell Biochem*. 2010;111(5):1222-1230.

49. Cochlear Implantation Work Guide. Guideline of cochlear implant (2013). *Zhonghua Yi Xue Hui*. 2014;49(2):89.

SUPPORTING INFORMATION

Additional supporting information can be found online in the Supporting Information section at the end of this article.